



Cite this: *Phys. Chem. Chem. Phys.*,  
2015, 17, 4076

# Kinetics of stabilised Criegee intermediates derived from alkene ozonolysis: reactions with SO<sub>2</sub>, H<sub>2</sub>O and decomposition under boundary layer conditions

Mike J. Newland,<sup>a</sup> Andrew R. Rickard,<sup>b</sup> Mohammed S. Alam,<sup>a</sup> Luc Vereecken,<sup>c</sup> Amalia Muñoz,<sup>d</sup> Milagros Ródenas<sup>d</sup> and William J. Bloss<sup>\*a</sup>

The removal of SO<sub>2</sub> in the presence of alkene–ozone systems has been studied for ethene, *cis*-but-2-ene, *trans*-but-2-ene and 2,3-dimethyl-but-2-ene, as a function of humidity, under atmospheric boundary layer conditions. The SO<sub>2</sub> removal displays a clear dependence on relative humidity for all four alkene–ozone systems confirming a significant reaction for stabilised Criegee intermediates (SCI) with H<sub>2</sub>O. The observed SO<sub>2</sub> removal kinetics are consistent with relative rate constants,  $k(\text{SCI} + \text{H}_2\text{O})/k(\text{SCI} + \text{SO}_2)$ , of  $3.3 (\pm 1.1) \times 10^{-5}$  for CH<sub>2</sub>OO,  $26 (\pm 10) \times 10^{-5}$  for CH<sub>3</sub>CHOO derived from *cis*-but-2-ene,  $33 (\pm 10) \times 10^{-5}$  for CH<sub>3</sub>CHOO derived from *trans*-but-2-ene, and  $8.7 (\pm 2.5) \times 10^{-5}$  for (CH<sub>3</sub>)<sub>2</sub>COO derived from 2,3-dimethyl-but-2-ene. The relative rate constants for  $k(\text{SCI decomposition})/k(\text{SCI} + \text{SO}_2)$  are  $-2.3 (\pm 3.5) \times 10^{11} \text{ cm}^{-3}$  for CH<sub>2</sub>OO,  $13 (\pm 43) \times 10^{11} \text{ cm}^{-3}$  for CH<sub>3</sub>CHOO derived from *cis*-but-2-ene,  $-14 (\pm 31) \times 10^{11} \text{ cm}^{-3}$  for CH<sub>3</sub>CHOO derived from *trans*-but-2-ene and  $63 (\pm 14) \times 10^{11} \text{ cm}^{-3}$  for (CH<sub>3</sub>)<sub>2</sub>COO. Uncertainties are  $\pm 2\sigma$  and represent combined systematic and precision components. These values are derived following the approximation that a single SCI is present for each system; a more comprehensive interpretation, explicitly considering the differing reactivity for *syn*- and *anti*-SCI conformers, is also presented. This yields values of  $3.5 (\pm 3.1) \times 10^{-4}$  for  $k(\text{SCI} + \text{H}_2\text{O})/k(\text{SCI} + \text{SO}_2)$  of *anti*-CH<sub>3</sub>CHOO and  $1.2 (\pm 1.1) \times 10^{13}$  for  $k(\text{SCI decomposition})/k(\text{SCI} + \text{SO}_2)$  of *syn*-CH<sub>3</sub>CHOO. The reaction of the water dimer with CH<sub>2</sub>OO is also considered, with a derived value for  $k(\text{CH}_2\text{OO} + (\text{H}_2\text{O})_2)/k(\text{CH}_2\text{OO} + \text{SO}_2)$  of  $1.4 (\pm 1.8) \times 10^{-2}$ . The observed SO<sub>2</sub> removal rate constants, which technically represent upper limits, are consistent with decomposition being a significant, structure dependent, sink in the atmosphere for *syn*-SCI.

Received 17th September 2014,  
Accepted 23rd December 2014

DOI: 10.1039/c4cp04186k

www.rsc.org/pccp

## 1. Introduction

Atmospheric oxidation processes are central to understanding trace gas atmospheric composition, the abundance of air pollutants harmful to human health, crops and ecosystems, and the removal of reactive greenhouse gases such as methane. The principal atmospheric oxidants responsible for initiating the gas-phase degradation of volatile organic compounds (VOCs), NO<sub>x</sub> and SO<sub>2</sub> are OH, NO<sub>3</sub> and O<sub>3</sub>, with additional contributions from other species such as halogen atoms. Recent field measurements<sup>1</sup> in

a boreal forest have identified the presence of an additional oxidant species, removing SO<sub>2</sub> and producing H<sub>2</sub>SO<sub>4</sub>. The additional SO<sub>2</sub> oxidation observed was substantial (comparable to that due to OH radicals alone), and attributed to a product of alkene ozonolysis – the boreal forest environment being one in which substantial biogenic alkene emissions occur – suggested to be the stabilised Criegee intermediate (SCI). The gas-phase oxidation of SO<sub>2</sub> in the atmosphere is of interest to climate research as it leads to formation of H<sub>2</sub>SO<sub>4</sub>, contributing to new particle formation and sulphate aerosol loading, in competition with condensed phase oxidation.<sup>2</sup> A missing mechanism for the conversion of SO<sub>2</sub> to H<sub>2</sub>SO<sub>4</sub> could lead to model underestimation of the sulphate aerosol burden and affect radiative forcing calculations,<sup>3</sup> with corresponding implications for climate predictions. Enhanced SO<sub>2</sub> oxidation in alkene–ozone systems was first reported by Cox & Penkett<sup>4</sup> over forty years ago, however the precise reaction mechanism giving rise to this effect remains elusive. The “Criegee” ozonolysis reaction mechanism was first postulated in the 1940s.<sup>5</sup> It is now accepted that the ozone

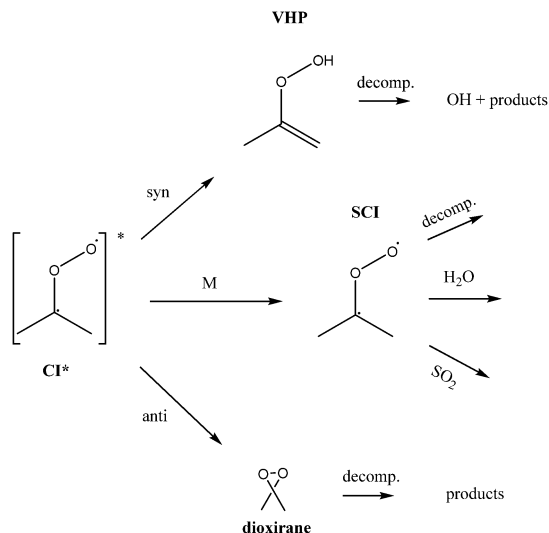
<sup>a</sup> University of Birmingham, School of Geography, Earth and Environmental Sciences, Birmingham, UK. E-mail: W.J.Bloss@bham.ac.uk

<sup>b</sup> Wolfson Atmospheric Chemistry Laboratories, Department of Chemistry, University of York, York, UK and National Centre for Atmospheric Science, University of York, York, UK

<sup>c</sup> Max Planck Institute for Chemistry, Atmospheric Sciences, J.-J.-Becher-Weg 27, Mainz, Belgium

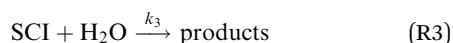
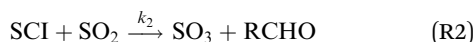
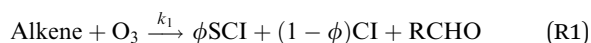
<sup>d</sup> Instituto Universitario CEAM-UMH, EUPHORE Laboratories, Avda/Charles R. Darwin. Parque Tecnológico, Valencia, Spain





**Scheme 1** Simplified mechanism for the reaction of Criegee Intermediates (SCIs) formed from alkene ozonolysis.

molecule adds to the C=C double bond *via* a concerted cyclo-addition to form a primary ozonide, followed by cleavage of the C–C bond and one of the O–O bonds forming a carbonyl molecule and a carbonyl oxide, or ‘Criegee intermediate’ (CI).<sup>6</sup> Ozonolysis derived SCIs are formed with a broad internal energy distribution, to yield chemically activated and stabilised SCIs. SCIs can have sufficiently long lifetimes to undergo bimolecular reactions with H<sub>2</sub>O and SO<sub>2</sub> amongst other species. Chemically activated SCIs may also undergo collisional stabilisation, unimolecular decomposition or isomerisation (Scheme 1). For substituted alkenes, SCIs can undergo a 1,4-H-shift rearrangement through a vinyl-hydroperoxide (VHP) *via* the so-called “hydroperoxide channel” and decompose to yield OH and a vinyloxy radical – a substantial non-photolytic source of atmospheric oxidants.<sup>7,8</sup> This is the favoured channel for SCIs formed in the *syn*-configuration. Time resolved studies<sup>9</sup> show that the VHP may persist for appreciable timescales under boundary layer conditions, giving rise to the observed pressure dependence of OH radical yields,<sup>10</sup> and opening the possibility for bimolecular reactions of this species to occur. SCIs formed in the *anti*-configuration are thought to primarily undergo rearrangement and decomposition *via* a dioxirane intermediate (“the acid/ester channel”), producing a range of daughter products and contributing to the observed overall HO<sub>x</sub> radical yield.<sup>6,11</sup>



Until recently, it has been thought that the predominant atmospheric fate for SCIs was reaction with water vapour<sup>12,13</sup> – leading to a significant source of organic acids and hydroperoxides,

suggesting that bimolecular reaction with SCIs is an unimportant oxidation mechanism for trace gas species. This view was recently challenged by direct observation<sup>14</sup> and kinetic studies<sup>15–17</sup> of the CH<sub>2</sub>OO and CH<sub>3</sub>CHOO SCIs.

Taatjes and co-workers,<sup>15</sup> directly observing CI kinetics for the first time, found reactions of CH<sub>2</sub>OO with SO<sub>2</sub> and NO<sub>2</sub> to be substantially faster than previously thought, pointing to a potentially important role for this species in atmospheric SO<sub>2</sub> and NO<sub>2</sub> oxidation; subsequent measurements have identified SO<sub>3</sub> (ref. 16) and NO<sub>3</sub> (ref. 18) as products of these reactions. The key to whether SCIs are indeed significant contributors to gas-phase atmospheric SO<sub>2</sub> oxidation is the ratio of the rate constants for reaction of the SCI with SO<sub>2</sub> ( $k_2$ ), to that with H<sub>2</sub>O ( $k_3$ ) and decomposition ( $k_4$ ). In laboratory studies where SCIs were produced by the 248 nm laser photolysis of alkyl iodide precursors at 4 Torr total pressure, with the SCI decay monitored by VUV photoionisation in the presence of excess co-reactants, this ratio has recently been reported to be 10<sup>3</sup>–10<sup>4</sup> for the smallest two SCIs (CH<sub>2</sub>OO<sup>15,17</sup> and CH<sub>3</sub>CHOO<sup>16</sup>), with  $k_2$  on the order of 10<sup>–11</sup> cm<sup>3</sup> s<sup>–1</sup> and  $k_3$  on the order of 10<sup>–15</sup> cm<sup>3</sup> s<sup>–1</sup>. In contrast, alternative studies of SO<sub>2</sub> oxidation in alkene–ozone systems, performed at atmospheric pressure through detection of the H<sub>2</sub>SO<sub>4</sub> product, find much smaller SCI + SO<sub>2</sub> rate coefficients (by *ca.* two orders of magnitude).<sup>19</sup> Explanations for this apparent discrepancy may include the lifetime of the secondary ozonide (SOZ) adduct formed from the SCI + SO<sub>2</sub> reaction, collisionally stabilised at atmospheric pressure,<sup>20</sup> effects of the presence of multiple SCI conformers with differing reactivity, or contributions from other oxidant species, formed within the ozonolysis system, to SO<sub>2</sub> reaction. Understanding the behaviour of the ozone–alkene–SO<sub>2</sub> system in the presence of water vapour is critical to quantifying the impact of SCI chemistry upon atmospheric SO<sub>2</sub> oxidation.<sup>21</sup>

An additional, potentially important, fate of SCI under atmospheric conditions is unimolecular decomposition (denoted  $k_4$  in (R4)). For CH<sub>2</sub>OO, rearrangement *via* a ‘hot’ acid species represents the lowest accessible decomposition channel, but due to lack of alkyl substituents, the theoretically predicted 298 K rate constant is rather low, 0.3 s<sup>–1</sup>.<sup>22</sup> Previous studies have identified the hydroperoxide rearrangement as dominant for SCIs with a *syn* configuration, determining their overall unimolecular decomposition rate.<sup>7,8</sup> For *syn*-CH<sub>3</sub>CHOO recent experimental<sup>23</sup> work yielded a decomposition rate of 3–30 s<sup>–1</sup>. Theoretical work<sup>24</sup> has predicted a decomposition rate coefficient of 24.2 s<sup>–1</sup> for *syn*-CH<sub>3</sub>CHOO and 67.2 s<sup>–1</sup> for *anti*-CH<sub>3</sub>CHOO (for which only the ester channel exists), owing to the potential energy release from the higher energy *anti*-conformer.<sup>23</sup> An upper limit to total CH<sub>3</sub>CHOO loss (decomposition and heterogeneous wall losses combined) of <250 s<sup>–1</sup> has been reported by Taatjes *et al.*<sup>16</sup> Earlier experimental work reported decomposition rate constants of ≤20 s<sup>–1</sup> for CH<sub>3</sub>CHOO derived from *cis*-but-2-ene ozonolysis,<sup>25</sup> and 76 s<sup>–1</sup> (accurate to within a factor of three) for CH<sub>3</sub>CHOO derived from *trans*-but-2-ene ozonolysis.<sup>26</sup> For (CH<sub>3</sub>)<sub>2</sub>COO (derived from 2,3-dimethyl-but-2-ene ozonolysis) a total loss rate of 3.0 s<sup>–1</sup> has recently been determined experimentally.<sup>19</sup> This value (which represents an upper limit for  $k_4$ )



is somewhat smaller than but comparable in magnitude to an earlier measurement of  $6.4 \text{ s}^{-1}$  (determined at 100 Torr).<sup>27</sup> Theoretical estimates of  $(\text{CH}_3)_2\text{COO}$  decomposition rates are higher, at up to  $250 \text{ s}^{-1}$ .<sup>22</sup> Photolysis loss rates have also recently been reported for  $\text{CH}_2\text{OO}$ <sup>28</sup> and  $\text{CH}_3\text{CHOO}$ <sup>29</sup> of  $1 \text{ s}^{-1}$  and  $0.2 \text{ s}^{-1}$  respectively, calculated for actinic flux values at midday,  $\text{SZA} = 0^\circ$ .

Here, we present results of a series of experiments in which the oxidation of  $\text{SO}_2$  during the ozonolysis of ethene, *cis*-but-2-ene, *trans*-but-2-ene and 2,3-dimethyl-but-2-ene (tetramethylethylene, TME), was investigated in the presence of varying amounts of water in the European Photochemical Reactor facility (EUPHORE), Valencia, Spain.

## 2. Experimental

### 2.1 EUPHORE

EUPHORE is a  $200 \text{ m}^3$  simulation chamber used for studying reaction mechanisms under atmospheric boundary layer conditions. In general, experiments comprised time-resolved measurement of the removal of  $\text{SO}_2$  in the presence of an alkene–ozone system, as a function of humidity.  $\text{SO}_2$  and  $\text{O}_3$  abundance were measured using conventional fluorescence and UV absorption monitors, respectively; alkene abundance was determined *via* FTIR spectroscopy. The precision of the  $\text{SO}_2$  and  $\text{O}_3$  monitors were 0.25 and 0.47 ppbv respectively (evaluated as 2 standard deviations of the measured value prior to  $\text{SO}_2$  or  $\text{O}_3$  addition). The chamber is fitted with large horizontal and vertical fans to ensure rapid mixing (three minutes). Further details of the chamber setup and instrumentation are available elsewhere.<sup>30,31</sup> Experiments were performed in the dark (*i.e.* with the chamber housing closed;  $j(\text{NO}_2) \leq 10^{-6} \text{ s}^{-1}$ ), at atmospheric pressure (*ca.* 1000 mbar) and temperatures between 296 and 303 K, on timescales of *ca.* 20–30 minutes. Chamber dilution was monitored *via* the first order decay of an aliquot of  $\text{SF}_6$ , added prior to each experiment. Cyclohexane (*ca.* 75 ppmv) was added at the beginning of each experiment to act as an OH scavenger, such that  $\text{SO}_2$  reaction with OH was calculated to be  $\leq 1\%$  of the total chemical  $\text{SO}_2$  removal in all experiments.

### 2.2 Experimental approach

Experimental procedure, starting with the chamber filled with clean air, comprised addition of  $\text{SF}_6$  and cyclohexane, followed by water vapour,  $\text{O}_3$  (*ca.* 500 ppbv) and  $\text{SO}_2$  (*ca.* 50 ppbv). A gap of five minutes was left prior to addition of the alkene, to allow complete mixing. The reaction was then initiated by addition of the alkene (*ca.* 500 ppbv for ethene, 200 ppbv for *cis*- and *trans*-but-2-ene and 400 ppbv for TME). The chamber was monitored for an hour subsequent to the addition of ethene and forty five minutes for *cis*- and *trans*-but-2-ene and TME. The rate of alkene–ozone consumption is dependent on  $k_1$ . Roughly 25% of the ethene was consumed after an hour, while for *cis*- and *trans*-but-2-ene and TME 90% of the alkene was consumed within roughly 25 minutes, 20 minutes and 6 minutes respectively. Each experiment was performed at a constant humidity, which was increased in a step-wise manner for consecutive runs to cover

the range 1.5–21% RH. Measured increases in  $[\text{SO}_2]$  agreed with measured volumetric addition across the  $\text{SO}_2$  and humidity range used in the experiments.

### 2.3 Analysis approach

The following sections describe (i) a common analysis applied to all systems, but which features several approximations, and (ii) more detailed consideration of each chemical system in turn, to address potential contributions from the water dimer, and multiple criegee species within each system (*e.g.* contrasting reactivity of different SCI conformers).

From the chemistry presented in reactions (R1)–(R4) it is assumed that SCI will be produced in the chamber from the reaction of the alkene with ozone at a given yield,  $\phi$ . The SCI produced can then react with  $\text{SO}_2$ , with  $\text{H}_2\text{O}$ , with other species or decompose under the experimental conditions applied. The rate at which  $\text{SO}_2$  is lost, compared with the total production of SCI, is determined by the fraction,  $f$ , of the total SCI produced which reacts with  $\text{SO}_2$ , compared to the sum of the total loss processes of the SCI (eqn (E1)):

$$f = \frac{k_2[\text{SO}_2]}{k_2[\text{SO}_2] + k_3[\text{H}_2\text{O}] + k_d + L} \quad (\text{E1})$$

$$\frac{d\text{SO}_2}{d\text{O}_3} = \phi \cdot f \quad (\text{E2})$$

Here,  $L$  is the sum of any other pseudo-first order chemical loss processes for SCI in the chamber, after correction for dilution. (E2) neglects other (non-alkene) chemical sinks for  $\text{O}_3$ , such as reaction with  $\text{HO}_2$  – also produced directly during alkene ozonolysis,<sup>11</sup> but indicated through model calculations to account for  $< 2\%$  of ozone loss under all the experimental conditions of this work. Eqn (E1) and (E2) treat the SCIs formed as a single species – this is the case for (*e.g.*) ethene and TME, but is an approximation for the 2-butenes; considered further below.

**2.3.1 SCI yield calculation.** Values for  $\phi_{\text{SCI}}$  were determined for each ozonolysis reaction from experiments performed under dry conditions ( $\text{RH} < 1\%$ ) in the presence of excess  $\text{SO}_2$  (*ca.* 1000 ppbv), such that  $\text{SO}_2$  scavenges the overwhelming majority of the SCI. From eqn (E2), regressing  $d\text{SO}_2$  against  $d\text{O}_3$  (corrected for chamber dilution), assuming  $f$  to be unity (*i.e.* all the SCI produced reacts with  $\text{SO}_2$ ) determines the value of  $\phi_{\text{min}}$ , a lower limit to the SCI yield. Fig. 2 shows the experimental data, from which  $\phi_{\text{min}}$  was derived, for all four alkene ozonolysis systems studied.

The lower limit criterion applies as in reality  $f$  will be less than one, at experimentally accessible  $\text{SO}_2$  levels, as a small fraction of the SCI will still react with any  $\text{H}_2\text{O}$  present, or undergo decomposition. The actual yield,  $\phi$ , was determined by combining the results from the high- $\text{SO}_2$  experiments with those from the series of experiments performed at lower  $\text{SO}_2$ , as a function of  $[\text{H}_2\text{O}]$ , to determine  $k_3/k_2$  and  $k_d/k_2$  (see Section 2.3.2), through an iterative process to determine the single unique value of  $\phi_{\text{SCI}}$  which fits both datasets. It is important to note that the SCI yield is to an extent an operationally defined quantity – for example, OH formation from alkene ozonolysis is known to proceed over



at least hundreds of milliseconds<sup>9</sup> following the alkene–ozone reaction, and so the corresponding CI population must also be evolving with time. In this work, SCI yields reflect the amount of SCI available to oxidise SO<sub>2</sub> on timescales of seconds to minutes.

**2.3.2  $k(\text{SCI} + \text{H}_2\text{O})/k(\text{SCI} + \text{SO}_2)$  and  $k_d/k(\text{SCI} + \text{SO}_2)$ .** To determine  $k_3/k_2$  and  $k_d/k_2$ , a series of experiments were performed for each alkene, in which the SO<sub>2</sub> loss was monitored as a function of [H<sub>2</sub>O]. From eqn (E2), regression of the loss of ozone ( $\Delta\text{O}_3$ ) against the loss of SO<sub>2</sub> ( $\Delta\text{SO}_2$ ) (both corrected for dilution, measured through the removal SF<sub>6</sub>, added at the start of each experiment and monitored *via* FTIR) for an experiment determines the factor  $f\phi$  at a given point in time. This quantity will vary through the experiment as SO<sub>2</sub> is consumed, and other potential SCI co-reactants are produced, as predicted by eqn (E1). A smoothed fit was applied to the experimental data for the cumulative consumption of SO<sub>2</sub> and O<sub>3</sub>,  $\Delta\text{SO}_2$  and  $\Delta\text{O}_3$ , (Fig. 1) to determine  $\text{dSO}_2/\text{dO}_3$  (and hence  $f\phi$ ) at the start of each experiment, for use in eqn (E3). The start of the experiment (*i.e.* when [SO<sub>2</sub>]  $\sim$  50 ppbv) was used as this corresponds to the greatest rate of production of the SCI, and hence largest experimental signals (O<sub>3</sub> and SO<sub>2</sub> rate of change) and is the point at which the SCI + SO<sub>2</sub> reaction has the greatest magnitude compared with any other potential chemical loss processes for either species (see discussion below).

$$[\text{SO}_2] \left( \frac{1}{f} - 1 \right) = \frac{k_3}{k_2} [\text{H}_2\text{O}] + \frac{k_d + L}{k_2} \quad (\text{E3})$$

The value  $[\text{SO}_2]((1/f) - 1)$  can then be regressed against [H<sub>2</sub>O] for each experiment to give a plot with a gradient of  $k_3/k_2$  and an intercept of  $(k_d + L)/k_2$  (eqn (E3)). Our data cannot determine absolute rate constants (*i.e.* values of  $k_2$ ,  $k_3$ ,  $k_d$ ) in isolation, but is limited to assessing their relative values, which may be placed on an absolute basis through use of an (external) reference value.

Eqn (E1)–(E3) as presented above assume that only a single SCI species is present in each ozonolysis system. While this is

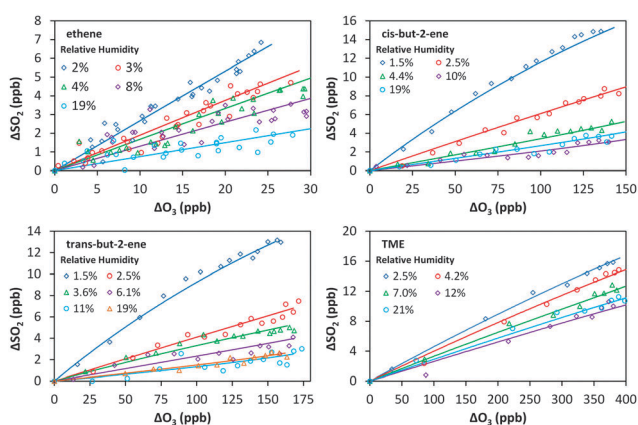


Fig. 1 Cumulative consumption of SO<sub>2</sub> and O<sub>3</sub>,  $\Delta\text{SO}_2$  versus  $\Delta\text{O}_3$ , for the ozonolysis of four alkenes in the presence of SO<sub>2</sub> at a range of relative humidities from 1.5–21%. Open symbols are experimental data, corrected for chamber dilution. Solid lines are smoothed fits to the experimental data.

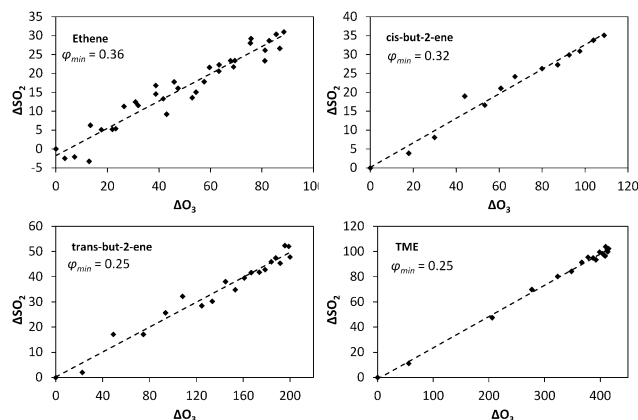


Fig. 2  $\Delta\text{SO}_2$  vs.  $\Delta\text{O}_3$  during the excess SO<sub>2</sub> experiments, to determine the minimum SCI yield for the four alkenes.

the case for the ethene and TME systems, for the but-2-ene systems this is an approximation as two conformers of the CH<sub>3</sub>CHO SCI (*syn* and *anti*) are produced. Further analysis is performed in Section 3.3.2 in which the SO<sub>2</sub> loss in the but-2-ene systems is treated as having two components, related to the different SCI.

## 3. Results and discussion

### 3.1 Introduction

Table 1 shows the resulting SCI yields obtained for the ozonolysis of ethene, *cis*-but-2-ene, *trans*-but-2-ene and tetramethylethylene (TME); uncertainties are  $\pm 2\sigma$ , and represent the combined systematic (estimated measurement uncertainty) and precision components. Also shown are past literature values, obtained under various conditions using a range of different SCI scavengers.

The yield of CH<sub>2</sub>OO from ethene ozonolysis obtained in this work is 0.37 ( $\pm 0.04$ ). This yield has been investigated in many previous studies, with values ranging from 0.34–0.50 determined – a more detailed review is available elsewhere.<sup>31</sup> The yield obtained in this work is at the lower end of but within the envelope of these estimates, and is in excellent agreement with the current IUPAC recommendation of 0.37.

The yield of CH<sub>3</sub>CHO from *cis*-but-2-ene ozonolysis obtained in this work is 0.38 ( $\pm 0.05$ ), with that from *trans*-but-2-ene being 0.28 ( $\pm 0.03$ ). These values fall within the range of reported literature values of 0.18–0.43 and 0.13–0.53 for *cis*-but-2-ene and *trans*-but-2-ene respectively (Table 1). *cis* and *trans*-but-2-ene both yield (differing) mixtures of *syn* and *anti* conformers of CH<sub>3</sub>CHO, the relative amounts of which are not well known, and which are treated here initially as a single SCI species (this approximation is discussed further in Section 3.3). Berndt *et al.*<sup>32</sup> recently reported a yield of 0.49 ( $\pm 0.22$ ) for the CH<sub>3</sub>CHO produced from *trans*-but-2-ene ozonolysis (also treating both *syn* and *anti* conformers as a single SCI species).

The yield of (CH<sub>3</sub>)<sub>2</sub>COO from TME ozonolysis obtained in this work is 0.32 ( $\pm 0.02$ ). This again falls within the (wide) range in the literature of 0.10–0.65, with Berndt *et al.*<sup>32</sup> most recently reporting a yield of 0.45 ( $\pm 0.20$ ).





**Table 1** SCI yields derived in this work and reported in the literature. Uncertainty ranges ( $\pm 2\sigma$ , parentheses) indicate combined precision and systematic measurement error components for this work, and are given as stated for literature studies. All referenced studies were conducted between 700 and 760 Torr. C2B – derived from *cis*-but-2-ene; T2B – derived from *trans*-but-2-ene

SCI	$\varphi_{\text{SCI}}$	Ref.
CH <sub>2</sub> OO	0.37 ( $\pm 0.04$ )	This work
	0.37	MCMv3.2 <sup>a</sup> (IUPAC) <sup>33</sup>
	0.35 ( $\pm 0.05$ )	Niki <i>et al.</i> <sup>34</sup>
	0.39 ( $\pm 0.053$ )	Hatakeyama <i>et al.</i> <sup>35</sup>
	0.47 ( $\pm 0.05$ )	Horie and Moortgat <sup>36</sup>
	0.50 ( $\pm 0.04$ )	Neeb <i>et al.</i> <sup>37</sup>
CH <sub>3</sub> CHOO (C2B)	0.38 ( $\pm 0.05$ )	This work
	0.19	Rickard <i>et al.</i> <sup>39</sup>
	0.18	Niki <i>et al.</i> <sup>40</sup>
	0.43	Cox and Penkett <sup>41</sup>
CH <sub>3</sub> CHOO (T2B)	0.28 ( $\pm 0.03$ )	This work
	0.49 ( $\pm 0.22$ )	Berndt <i>et al.</i> <sup>32</sup>
	0.53 ( $\pm 0.24$ )	Berndt <i>et al.</i> <sup>19</sup>
	0.45	Cox and Penkett <sup>41</sup>
	0.19 ( $\pm 0.03$ )	Hatakeyama <i>et al.</i> <sup>35</sup>
	0.42	Horie and Moortgat <sup>36</sup>
(CH <sub>3</sub> ) <sub>2</sub> COO	0.24 ( $\pm 0.07$ )	Hasson <i>et al.</i> <sup>38</sup>
	0.13	Rickard <i>et al.</i> <sup>39</sup>
	0.32 ( $\pm 0.02$ )	This work
	0.45 ( $\pm 0.20$ )	Berndt <i>et al.</i> <sup>32</sup>
	0.62 ( $\pm 0.28$ )	Berndt <i>et al.</i> <sup>19</sup>
	ca. 0.65 <sup>b</sup>	Drozd <i>et al.</i> <sup>10</sup>
	0.10 ( $\pm 0.03$ )	Hasson <i>et al.</i> <sup>38</sup>
	0.30	Niki <i>et al.</i> <sup>40</sup>
	0.11	Rickard <i>et al.</i> <sup>39</sup>

<sup>a</sup> <http://mcm.leeds.ac.uk/MCM/>. <sup>b</sup> At 700–760 Torr (low pressure limit of 0.15 at 0 Torr).

Fig. 1 shows the cumulative consumption of SO<sub>2</sub> relative to that of O<sub>3</sub>,  $\Delta\text{SO}_2$  versus  $\Delta\text{O}_3$  (after correction for dilution), as a function of [H<sub>2</sub>O] for each experiment for the four alkenes studied. A fit to each experiment, extrapolating the experimental data to evaluate  $d\text{SO}_2/d\text{O}_3$  at  $t = 0$  (start of each experimental run) for use in eqn (E1)–(E3), is also shown. The overall change in SO<sub>2</sub>,  $\Delta\text{SO}_2$ , is seen to decrease substantially with increasing humidity (over a relatively narrow range of RH (1.5–20%)) for all four alkenes. This trend would be expected from the understood chemistry ((R1)–(R4)), as there is competition between SO<sub>2</sub>, H<sub>2</sub>O, and decomposition for reaction with the SCI.

Fig. 3 shows a fit of eqn (E3) to the data for each alkene, giving a slope of  $k_3/k_2$ , and an intercept of  $(k_d + L)/k_2$ . The results appear to show a generally linear relationship; however, for *cis*- and *trans*-but-2-ene and TME, the data point at the highest relative humidity accessible in this work ([H<sub>2</sub>O] = 1.5–2.0 × 10<sup>17</sup> cm<sup>-3</sup>) appears to deviate from this relationship. These data points lie outside the 95% confidence intervals defined by all the other (lower relative humidity) data for each alkene. For the analysis to determine  $k_3/k_2$  and  $(k_d + L)/k_2$  presented in Table 2, the points at the highest RH are excluded and the kinetic parameters are derived from a linear fit to the measurements from all other experiments. Extended analyses to account for the non-linearity

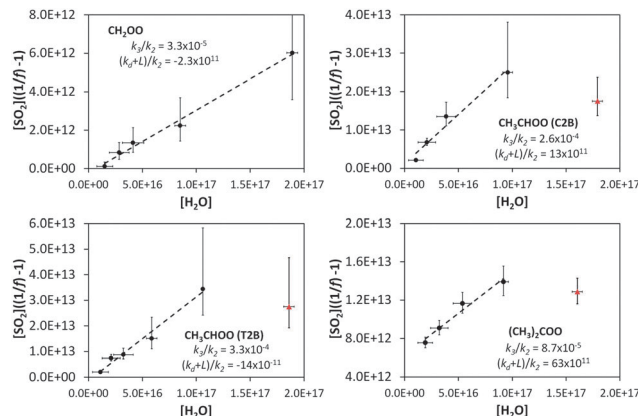


**Fig. 3** Application of eqn (E3) to derive rate constants for reaction of CH<sub>2</sub>OO, CH<sub>3</sub>CHOO (derived from *cis*-but-2-ene; C2B), CH<sub>3</sub>CHOO (derived from *trans*-but-2-ene; T2B), and (CH<sub>3</sub>)<sub>2</sub>COO with H<sub>2</sub>O ( $k_3$ ) and decomposition ( $k_d$ ), relative to that for reaction with SO<sub>2</sub>,  $k_3/k_2$  and  $(k_d + L)/k_2$  – see text.

**Table 2** SCI relative rate constants derived in this work using the single-SCI water monomer approach (*i.e.* eqn (E3); see text). Uncertainty ranges ( $\pm 2\sigma$ , parentheses) indicate combined precision and systematic measurement error components

SCI	10 <sup>5</sup> $k_3/k_2$	10 <sup>-11</sup> cm <sup>-3</sup> $k_d/k_2$
CH <sub>2</sub> OO	3.3 ( $\pm 1.1$ )	-2.3 ( $\pm 3.5$ )
CH <sub>3</sub> CHOO (C2B)	26 ( $\pm 10$ )	13 ( $\pm 43$ )
CH <sub>3</sub> CHOO (T2B)	33 ( $\pm 10$ )	-14 ( $\pm 31$ )
(CH <sub>3</sub> ) <sub>2</sub> COO	8.7 ( $\pm 2.5$ )	63 ( $\pm 14$ )

observed for CH<sub>3</sub>CHOO and (CH<sub>3</sub>)<sub>2</sub>COO are presented in the following sections.

One potential explanation for the observed curvature in the CH<sub>3</sub>CHOO and (CH<sub>3</sub>)<sub>2</sub>COO data is measurement error.  $\Delta\text{SO}_2$  is relatively small at high [H<sub>2</sub>O] compared to the precision of the measurements; however, even allowing for associated uncertainties, the points at high RH do not fit the linear relationship successfully applied to the remaining data points. Moreover, any systematic error in the measurement of O<sub>3</sub>, SO<sub>2</sub> or H<sub>2</sub>O would also be expected to affect the results for the ethene system (and to a greater extent, given the slow ethene–ozone reaction rate and consequent lower overall chemical SO<sub>2</sub> loss observed), suggesting that the cause lies in contrasting chemical behaviour. In terms of experimental factors, H<sub>2</sub>O was measured using multiple approaches (two dew-point hygrometers in addition to a solid state probe) with no evidence for any divergence with RH. SO<sub>2</sub> monitors can exhibit humidity-dependent interferences (quenching of the SO<sub>2</sub> signal), commonly of the order of a few percent, observed at very high RH, and corrected through incorporation of a nafion dryer (fitted in this case); in addition the monitor-derived SO<sub>2</sub> concentration increments were in agreement with those calculated from the measured SO<sub>2</sub> addition and chamber volume, across the relative humidity range studied.

It should be noted that the  $k_d$  values reported here represent upper limits, as a consequence of possible further chemical losses for the SCI within our experimental system (as represented by  $L$  in eqn (E3), notwithstanding the approach of extrapolating to the start of each experiment to minimise these). Other potential



fates for SCIs include reaction with ozone,<sup>42,43</sup> other SCI,<sup>43</sup> carbonyl products,<sup>44</sup> acids,<sup>45</sup> or with the parent alkene<sup>43</sup> itself. Sensitivity analyses indicate that the reaction with ozone could be significant, as predicted by theory<sup>42,43</sup> with a possible contribution of up to 10% of SCI loss for (CH<sub>3</sub>)<sub>2</sub>COO at 2% RH, while total losses from reaction with SCI (self-reaction), carbonyls and alkenes are calculated to account for <1% of the total SCI loss under the experimental conditions applied.

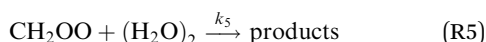
### 3.2 CH<sub>2</sub>OO

**3.2.1 Linear Fit.** For CH<sub>2</sub>OO a linear fit (*i.e.* using eqn (E3) vs. H<sub>2</sub>O) describes the observations well (Fig. 3) over the entire [H<sub>2</sub>O] range studied (1–20 × 10<sup>16</sup> molecules per cm<sup>-3</sup>). This fit gives relative rates  $k_3/k_2$  of 3.3 (±1.1) × 10<sup>-5</sup> and  $(k_d + L)/k_2$  of -2.3 (±3.5) × 10<sup>11</sup> cm<sup>-3</sup> (Table 2).

These relative rates can be placed on an absolute basis using absolute measurements of  $k_2(\text{SCI} + \text{SO}_2)$ . In Table 3 we apply the absolute  $k_2$  values reported by Welz *et al.*,<sup>15</sup> obtained using direct methods at reduced pressure (4 Torr), to the relative rates shown in Table 2. Using this method, the value obtained for  $k_3(\text{CH}_2\text{OO} + \text{H}_2\text{O})$  is 1.3 (±0.4) × 10<sup>-15</sup> cm<sup>3</sup> s<sup>-1</sup>. This is consistent with the recent determination by Welz *et al.*,<sup>15</sup> that  $k_3 < 4 \times 10^{-15}$  cm<sup>3</sup> s<sup>-1</sup>, but is (*ca.* 14–50 times) greater than the recent estimates of Ouyang *et al.*<sup>18</sup> ( $k_3 = 2.5 (\pm 1) \times 10^{-17}$  cm<sup>3</sup> s<sup>-1</sup>) and Stone *et al.*<sup>17</sup> ( $k_3 < 9 \times 10^{-17}$  cm<sup>3</sup> s<sup>-1</sup>).

The derived  $(k_d + L)$  value for CH<sub>2</sub>OO using this method is -8.8 (±13) s<sup>-1</sup>, *i.e.* zero within uncertainty. Theoretical work<sup>22</sup> has predicted  $k_d(\text{CH}_2\text{OO})$  to be small (~0.3 s<sup>-1</sup>), in agreement with the experimentally derived value reported here.

**3.2.2 CH<sub>2</sub>OO + (H<sub>2</sub>O)<sub>2</sub>.** Recent experimental work<sup>46</sup> has reported the reaction of CH<sub>2</sub>OO with the water dimer, (H<sub>2</sub>O)<sub>2</sub>, (reaction (R5)) to be very fast (1.1 × 10<sup>-11</sup> cm<sup>3</sup> s<sup>-1</sup> – assuming  $k_2 = 3.9 \times 10^{-11}$  cm<sup>3</sup> s<sup>-1</sup> (ref. 15)), in broad agreement with theoretical predictions,<sup>47</sup> but in contrast to other experimental work.<sup>45</sup>



The CH<sub>2</sub>OO data from this study appear to be well described by a linear fit under the experimental conditions applied

(a fast reaction of CH<sub>2</sub>OO with (H<sub>2</sub>O)<sub>2</sub> would be manifested as a significant upward curvature in Fig. 3). However, this does not mean the results are inconsistent with reaction of CH<sub>2</sub>OO with (H<sub>2</sub>O)<sub>2</sub>.

In Fig. 4, eqn (E4) (an expanded version of eqn (E3), including the SCI + (H<sub>2</sub>O)<sub>2</sub> reaction (R5)) is applied to the data, now expressed in terms of (H<sub>2</sub>O)<sub>2</sub>, calculated for each RH *via* the equilibrium constant.<sup>48</sup>

$$[\text{SO}_2]_0 \left( \frac{1}{f} - 1 \right) = \frac{k_3}{k_2} \sqrt{\frac{[(\text{H}_2\text{O})_2]}{K_p}} + \frac{k_5}{k_2} [(\text{H}_2\text{O})_2] + \frac{k_d}{k_2} \quad (\text{E4})$$

The value for  $k_3/k_2$  (water monomer) derived from the fit shown in Fig. 4 is 2.5 (±0.7) × 10<sup>-5</sup>. It is seen that this value is rather insensitive to the inclusion of the (H<sub>2</sub>O)<sub>2</sub> term in eqn (E4) as the value is within the uncertainties of the linear fit to the data presented in Fig. 3 – see also Table 2. Converting this value to an absolute value using the  $k_2$  from Welz *et al.*<sup>15</sup> gives  $k_3 = 9.9 (\pm 2.9) \times 10^{-16}$  cm<sup>3</sup> s<sup>-1</sup>. The derived value of  $k_d/k_2$  is -6.4 (±66) × 10<sup>10</sup> cm<sup>-3</sup>, which, using the Welz *et al.*<sup>15</sup>  $k_2$  gives an absolute value for  $k_d$  of -1.5 (±16) s<sup>-1</sup>. This is again indistinguishable from zero, within uncertainty, as is the  $k_d$  determined from eqn (E3) (Fig. 3). Note the large uncertainties in  $k_d$ , resulting from allowing three parameters to vary in the optimisation; consequently  $k_d$  was fixed to zero in eqn (E4) to determine the  $k_3/k_2$  and  $k_5/k_2$  values.

The resulting value of  $k_5/k_2$  (water dimer) is 1.4 (±1.8) × 10<sup>-2</sup>. Converting this to an absolute value using the  $k_2$  from Welz *et al.*<sup>15</sup> gives  $k_5 = 5.6 (\pm 7.0) \times 10^{-13}$  cm<sup>3</sup> s<sup>-1</sup>. This is roughly a factor of twenty smaller than the value derived by Berndt *et al.*,<sup>46</sup> but within a factor of two of the upper limit for  $k_5$  deduced by Welz *et al.* (<3 × 10<sup>-13</sup> cm<sup>3</sup> s<sup>-1</sup>) (ref. 45) from the data presented by Stone *et al.*<sup>17</sup> The inset plot in Fig. 4 also shows two additional fits generated using eqn (E4) with  $k_3/k_2$  fixed to 9.9 × 10<sup>-16</sup> and  $k_d$  fixed to zero. One fit line uses the  $k_5$  value reported by Berndt *et al.*<sup>46</sup> (blue dashed line). This is seen to overestimate the presented data. The green dotted line shows a fit to the upper limits of the uncertainties of the measured data. This yields a  $k_5/k_2$  value of 0.10 (±0.01), giving an upper limit  $k_5$  value of 3.9 (±0.39) × 10<sup>-12</sup> cm<sup>3</sup> s<sup>-1</sup>.

**Table 3** Comparison of SCI relative rate constants derived in this work to relative and absolute values from the literature. Uncertainty ranges (±2σ) indicate combined precision and systematic measurement error components

SCI	10 <sup>5</sup> $k_3/k_2$	10 <sup>15</sup> $k_3$ (cm <sup>3</sup> s <sup>-1</sup> )	10 <sup>-11</sup> $k_d/k_2$ (cm <sup>-3</sup> )	$k_d$ (s <sup>-1</sup> )	Ref.	Method	Conditions <sup>a</sup>
CH <sub>2</sub> OO	3.3 (±1.1)	1.3 (±0.4) <sup>b</sup>	-2.3 (±3.5)	-8.8 (±13) <sup>b</sup>	This work	Ethene ozonolysis	298–303 K
		<4			Welz <i>et al.</i> <sup>15</sup>	Alkyl iodide photolysis	4 Torr; 298 K
		<0.09			Stone <i>et al.</i> <sup>17</sup>	Alkyl iodide photolysis	200 Torr; 295 K
CH <sub>3</sub> CHOO	26 (±10)	12 (±4.5) <sup>c</sup>	13 (±43)	59 (±196) <sup>c</sup>	This work	C2B ozonolysis	296–302 K
	33 (±10)	15 (±4.5) <sup>c</sup>	-14 (±31)	-64 (±141) <sup>c</sup>	This work	T2B ozonolysis	297–302 K
		<i>anti</i> 10 (±4); <i>syn</i> <4			Taatjes <i>et al.</i> <sup>16</sup>	Alkyl iodide photolysis	4 Torr; 298 K
	8.8 (±0.4)		12 (±0.1)		Berndt <i>et al.</i> <sup>32</sup>	T2B ozonolysis	293 K
				Fenske <i>et al.</i> <sup>26</sup>	T2B ozonolysis	296 K	
(CH <sub>3</sub> ) <sub>2</sub> COO	8.7 (±2.5)	2.1 (±0.6) <sup>d</sup>	63 (±14)	151 (±35) <sup>d</sup>	This work	TME ozonolysis	298–299 K
	<0.4		42 (±3)		Berndt <i>et al.</i> <sup>32</sup>	TME ozonolysis	293 K

<sup>a</sup> Experiments were conducted at atmospheric pressure unless stated otherwise. <sup>b</sup> Assuming  $k_2 = 3.9 \times 10^{-11}$  cm<sup>3</sup> s<sup>-1</sup> (Welz *et al.*<sup>15</sup>). <sup>c</sup> Assuming  $k_2 = 4.55 \times 10^{-11}$  cm<sup>3</sup> s<sup>-1</sup>. Average of  $k_2$  for *syn* and *anti* CH<sub>3</sub>CHOO conformers from Taatjes *et al.*<sup>16</sup> <sup>d</sup> Assuming  $k_2 = 2.4 \times 10^{-11}$  cm<sup>3</sup> s<sup>-1</sup>.  $k_2$  for *syn*-CH<sub>3</sub>CHOO from Taatjes *et al.*<sup>16</sup>



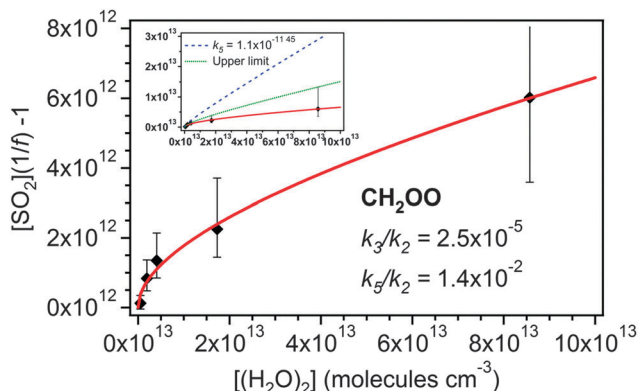


Fig. 4 Application of eqn (E4) to derive rate constants for reaction of  $\text{CH}_2\text{OO}$  with  $\text{H}_2\text{O}$  ( $k_3/k_2$ ) and  $(\text{H}_2\text{O})_2$  ( $k_5/k_2$ ) relative to that of  $\text{CH}_2\text{OO}$  with  $\text{SO}_2$ . Inset: eqn (E4) as shown in the main figure (red line), (E4) applied using the dimer reaction rate ( $k_5$ ) reported by Berndt *et al.*<sup>45</sup> ( $1.1 \times 10^{-11} \text{ cm}^3 \text{ s}^{-1}$ ) (dashed line) and a fit to the upper limits of the uncertainties in the ethene data (solid green line).

The contribution of  $(\text{H}_2\text{O})_2$  to the removal of  $\text{CH}_2\text{OO}$  increases in relation to that of  $\text{H}_2\text{O}$  as  $[\text{H}_2\text{O}]$  increases. Hence at typical atmospheric  $[\text{H}_2\text{O}]$  ( $\sim 2.5\text{--}7.5 \times 10^{17} \text{ molecules per cm}^{-3}$ ), greater than was accessible in this study, reaction with  $(\text{H}_2\text{O})_2$  could become the dominant sink for  $\text{CH}_2\text{OO}$ . In this case using just the  $\text{H}_2\text{O}$  monomer kinetics in models would considerably underestimate the total effect of water on removal of  $\text{CH}_2\text{OO}$  in the atmosphere.

### 3.3 $\text{CH}_3\text{CHOO}$

**3.3.1 Single SCI Approach.** The  $\text{CH}_3\text{CHOO}$  data shown in Fig. 3 for both *cis* and *trans*-but-2-ene appear to be well described (within the uncertainties) by a linear fit to eqn (E3), with the exception of the experiment at the highest RH ( $[\text{H}_2\text{O}] = 1.8\text{--}1.9 \times 10^{17} \text{ cm}^{-3}$ ) in both cases. The kinetic parameters derived from a linear fit to the data (Fig. 3), using eqn (E3) (which treats the system as producing a single SCI), excluding the highest RH experiments, are shown in Table 2. Very similar results are obtained for  $k_3/k_2$  for  $\text{CH}_3\text{CHOO}$  derived from both *cis*- and *trans*-but-2-ene ozonolysis, with values of  $26 (\pm 10) \times 10^{-5}$  and  $33 (\pm 10) \times 10^{-5}$  respectively. The  $(k_d + L)/k_2$  obtained for  $\text{CH}_3\text{CHOO}$  from *cis*-but-2-ene ozonolysis is  $13 (\pm 43) \times 10^{11} \text{ molecule cm}^{-3}$  and from *trans*-but-2-ene ozonolysis  $-14 (\pm 31) \times 10^{11} \text{ molecule cm}^{-3}$ . Berndt *et al.*<sup>32</sup> reported the  $k_3/k_2$  ratio from *trans*-but-2-ene ozonolysis to be  $8.8 (\pm 0.4) \times 10^{-5}$  (also assuming a single SCI system), a factor of 3.75 smaller than that reported here.

The relative rate constants (Table 2) can be placed on an absolute basis using the measurements of  $k_2(\text{SCI} + \text{SO}_2)$  reported by Taatjes *et al.*<sup>16</sup> (derived using the same methodology as for  $\text{CH}_2\text{OO}$ ) (Table 3). As eqn (E3) treats the SCI produced as a single SCI, we use an average of the *syn* and *anti* conformer rates presented in Taatjes *et al.*,<sup>16</sup>  $4.55 \times 10^{-11} \text{ cm}^3 \text{ s}^{-1}$ . Using this method, the value obtained for  $k_3(\text{CH}_3\text{CHOO} + \text{H}_2\text{O})$  from *cis*-but-2-ene ozonolysis is  $12 (\pm 4.5) \times 10^{-15} \text{ cm}^3 \text{ s}^{-1}$  and from *trans*-but-2-ene ozonolysis is  $15 (\pm 4.5) \times 10^{-15} \text{ cm}^3 \text{ s}^{-1}$ . Taking a mean of the  $k_3$  values reported for the two  $\text{CH}_3\text{CHOO}$  conformers

by Taatjes *et al.*<sup>16</sup> gives a value of  $7.0 \times 10^{-15} \text{ cm}^3 \text{ s}^{-1}$ , while Sheps *et al.*<sup>49</sup> give a mean value of  $12 \times 10^{-15} \text{ cm}^3 \text{ s}^{-1}$ . The values obtained for  $(k_d + L)$  are  $59 (\pm 196) \text{ s}^{-1}$  from *cis*-but-2-ene and  $-64 (\pm 141) \text{ s}^{-1}$  from *trans*-but-2-ene. Clearly there is a large uncertainty associated with the  $k_d$  determined from this analysis. Fenske *et al.*<sup>26</sup> have reported  $k_d(\text{CH}_3\text{CHOO})$  from *trans*-but-2-ene ozonolysis to be  $76 \text{ s}^{-1}$  (accurate to within a factor of three).

**3.2.2 Two conformer system.** In Fig. 1 it is evident that  $\text{dSO}_2/\text{dO}_3$  falls rapidly with increasing  $[\text{H}_2\text{O}]$  for all but-2-ene experiments as RH is initially increased, but that the experiments at higher RH all appear to display a similar  $\text{dSO}_2/\text{dO}_3$ , *i.e.* the trend in decreasing  $\text{SO}_2$  removal with increasing  $\text{H}_2\text{O}$  levels off. From this observation it appears that there may be competing  $\text{H}_2\text{O}$  dependencies to the  $\text{SO}_2$  loss present. This is manifested in Fig. 3 as a curving over of the data at high RH. We propose two possible explanations for this observation: firstly that it arises from differing kinetics of the two  $\text{CH}_3\text{CHOO}$  conformers formed in but-2-ene ozonolysis; secondly that the behaviour may reflect the presence of an additional oxidant being formed in the ozonolysis system that reacts with  $\text{SO}_2$  but is less sensitive to  $\text{H}_2\text{O}$ . The first of these possibilities is discussed below, the second is discussed in relation to  $(\text{CH}_3)_2\text{COO}$  in the following section.

One explanation for the observed non-linearity at high RH apparent in Fig. 3 is the differing reactivities of the *syn*- and *anti*-conformers of  $\text{CH}_3\text{CHOO}$  produced in the ozonolysis of *cis*- and *trans*-but-2-ene. It has been predicted<sup>50</sup> that the *anti*-conformer reacts with  $\text{H}_2\text{O}$  several orders of magnitude faster than the *syn*-conformer, while the rate constant for the SCI reaction with  $\text{SO}_2$  has been determined experimentally<sup>16</sup> to be about a factor of three greater for the *anti*-conformer than the *syn*-conformer. The fraction of each conformer that is lost to reaction with  $\text{SO}_2$  can be considered in the same way as illustrated in eqn (E2), leading to eqn (E5) and (E6) below, plus simplifications outlined in the following text. The total loss of  $\text{SO}_2$  to  $\text{CH}_3\text{CHOO}$  is then the sum of the fractional loss to each conformer, multiplied by the relative SCI yield ( $\gamma$ ) (*i.e.*  $\phi^{\text{syn}}/\phi$ ) of that conformer (eqn (E7)).

$$f^{\text{syn}} = \frac{[\text{SO}_2]}{[\text{SO}_2] + \frac{k_3^{\text{syn}}}{k_2^{\text{syn}}}[\text{H}_2\text{O}] + \frac{k_d^{\text{syn}}}{k_2^{\text{syn}}}} \approx \frac{[\text{SO}_2]}{[\text{SO}_2] + \frac{k_d^{\text{syn}}}{k_2^{\text{syn}}}} \quad (\text{E5})$$

$$f^{\text{anti}} = \frac{[\text{SO}_2]}{[\text{SO}_2] + \frac{k_3^{\text{anti}}}{k_2^{\text{anti}}}[\text{H}_2\text{O}] + \frac{k_d^{\text{anti}}}{k_2^{\text{anti}}}} \approx \frac{[\text{SO}_2]}{[\text{SO}_2] + \frac{k_3^{\text{anti}}}{k_2^{\text{anti}}}[\text{H}_2\text{O}]} \quad (\text{E6})$$

$$f = \gamma^{\text{syn}} f^{\text{syn}} + \gamma^{\text{anti}} f^{\text{anti}} \quad (\text{E7})$$

Eqn (E8) can then be fitted to the data presented in Fig. 3 for *cis*- and *trans*-but-2-ene (Fig. 5).

$$[\text{SO}_2] \left( \frac{1}{f} - 1 \right) = [\text{SO}_2] \left( \frac{1}{\gamma^{\text{syn}} f^{\text{syn}} + \gamma^{\text{anti}} f^{\text{anti}}} - 1 \right) \quad (\text{E8})$$

Here we make two assumptions to reduce the degrees of freedom and hence make the problem tractable with the



dataset available. First it is assumed that  $k_3^{syn}[\text{H}_2\text{O}]$  may be neglected, in keeping with theoretical predictions<sup>24</sup> predicting  $k_d^{syn}$  to be over three orders of magnitude greater than  $k_3^{syn}[\text{H}_2\text{O}]$ . Further theoretical work<sup>50</sup> predicts a rate constant for  $\text{syn-CH}_3\text{CHOO} + \text{H}_2\text{O}$  of  $2.39 \times 10^{-18} \text{ cm}^3 \text{ s}^{-1}$ , and recent experimental work<sup>49</sup> yields an upper limit for  $k_3^{syn}$  of  $< 2 \times 10^{-16} \text{ cm}^3 \text{ s}^{-1}$ . Hence with  $k_d^{syn}$  expected to be relatively fast, given the decomposition rate presented here for  $(\text{CH}_3)_2\text{COO}$  (a *syn*-conformer) and the facile decomposition route available *via* the hydroperoxide mechanism for the *syn*-conformer, it can be assumed that  $k_d^{syn} \gg k_3^{syn}[\text{H}_2\text{O}]$  at the experimental conditions reported here. Second it is assumed that  $k_d^{anti} \ll k_3^{anti}[\text{H}_2\text{O}]$  under the experimental conditions used. If the kinetics derived from treating the but-2-ene data in Fig. 3 as representing a single SCI are dominated by the *anti*-conformer then the  $k_d$  derived from these kinetics, which is indistinguishable from zero within the uncertainties, suggests that  $k_d^{anti}$  is small. Taatjes *et al.*<sup>16</sup> report  $k_3^{anti}$  to be  $1.0 (\pm 0.4) \times 10^{-14} \text{ cm}^3 \text{ s}^{-1}$ , while Sheps *et al.*<sup>49</sup> report a value of  $2.4 (\pm 0.4) \times 10^{-14} \text{ cm}^3 \text{ s}^{-1}$ . Thus, even at the lowest  $[\text{H}_2\text{O}]$  considered here ( $\sim 1 \times 10^{16} \text{ cm}^{-3}$ ), loss of *anti-CH}\_3\text{CHOO} to  $\text{H}_2\text{O}$  would be  $> 100 \text{ s}^{-1}$ , and decomposition negligible in comparison (including a  $k_d^{anti}$  of  $50 \text{ s}^{-1}$  changes the derived  $k_3^{anti}$  and  $k_d^{syn}$  values by  $< 5\%$ ).*

Fitting eqn (E8) to the data shown in Fig. 5 derives a range of values for  $k_3^{anti}$  and  $k_d^{syn}$  dependent on the values of  $\gamma^{anti}$  and  $\gamma^{syn}$  used. As the CIs, once formed and thermalised, are expected to show the same kinetic behaviour in these experiments irrespective

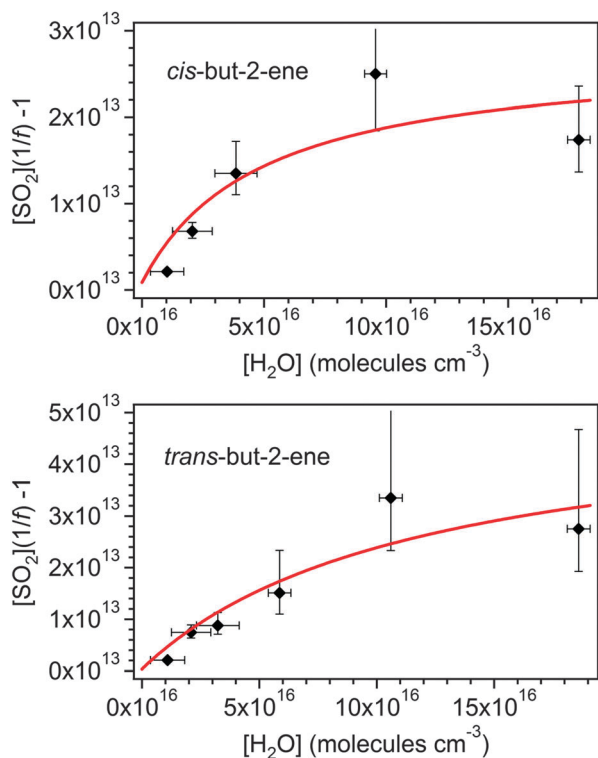


Fig. 5 Fits of eqn (E8) to the *cis*-but-2-ene and *trans*-but-2-ene data shown in Fig. 3.  $\gamma^{syn}$  and  $\gamma^{anti}$  are 0.45 and 0.55 for *cis*-but-2-ene and 0.25 and 0.75 for *trans*-but-2-ene (see Fig. 6).

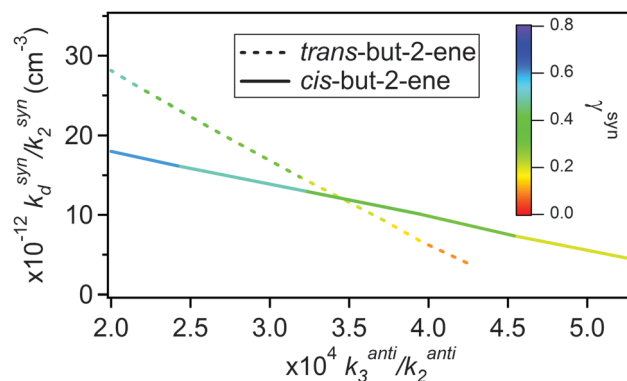


Fig. 6 The ranges of  $k_3^{anti}/k_2^{anti}$  and  $k_d^{syn}/k_2^{syn}$  determined from fitting eqn (E8) to the but-2-ene data (Fig. 5). The colour legend shows the fraction of the total  $\text{CH}_3\text{CHOO}$  formed that is *syn-CH}\_3\text{CHOO} ( $\gamma^{syn}$ ).*

of their precursor alkene, the measurements from the *cis*-but-2-ene and *trans*-but-2-ene experiments can be used in combination to constrain  $k_3^{anti}$ ,  $k_d^{syn}$  and also  $\gamma^{syn}$  and  $\gamma^{anti}$  from each alkene. Fig. 6 plots the  $k_3^{anti}$  vs.  $k_d^{syn}$  determined at different  $\gamma^{syn}$  and  $\gamma^{anti}$  from *cis*-but-2-ene and *trans*-but-2-ene. Where these two lines intercept represents the unique solution for both  $k_3^{anti}$  and  $k_d^{syn}$  and for  $\gamma^{syn}$  and  $\gamma^{anti}$  (Table 4).

Fig. 6 determines  $k_3^{anti}/k_2^{anti}$  to be  $3.5 (\pm 3.1) \times 10^{-4}$  and  $k_d^{syn}/k_2^{syn}$  to be  $1.2 (\pm 1.1) \times 10^{13} \text{ cm}^{-3}$ . The  $2\sigma$  uncertainties presented are, unsurprisingly, large as there are two free parameters. Using the relevant values of  $k_2$  for the *syn* and *anti-CH}\_3\text{CHOO} conformers from Taatjes *et al.*<sup>16</sup> to place the relative rate constants on an absolute basis gives a value for  $k_3^{anti}$  of  $2.3 (\pm 2.1) \times 10^{-14} \text{ cm}^3 \text{ s}^{-1}$  and for  $k_d^{syn}$  of  $288 (\pm 275) \text{ s}^{-1}$ . This  $k_3^{anti}$  is comparable to (a factor of two greater than) that reported by Taatjes *et al.*<sup>16</sup> ( $1.0 (\pm 0.4) \times 10^{-14}$ ). Novelli *et al.*<sup>23</sup> have recently reported  $k_d^{syn}$  to be an order of magnitude smaller ( $3\text{--}30 \text{ s}^{-1}$ ) based on direct observation of OH formation during *trans*-but-2-ene ozonolysis at atmospheric pressure.*

The point of interception in Fig. 6 also determines the relative yields of the two conformers,  $\gamma^{syn}$  and  $\gamma^{anti}$  (which in turn has been used to derive the optimised fits shown in Fig. 5). For *cis*-but-2-ene these are determined as 0.45 and 0.55 for  $\gamma^{syn}$  and  $\gamma^{anti}$  respectively. For *trans*-but-2-ene they are determined as 0.25 for  $\gamma^{syn}$  and 0.75 for  $\gamma^{anti}$ . The analysis performed in this section has implications for the determination of the SCI yield. Using the relative rate constant  $k_3/k_2(\text{anti-CH}_3\text{CHOO})$  obtained, as shown in Table 4, it is calculated that  $\sim 90\%$  of the *anti-CH}\_3\text{CHOO} produced in the SCI yield experiments would react with  $\text{SO}_2$ . From the determined  $k_d/k_2(\text{syn-CH}_3\text{CHOO})$  it is calculated that  $\sim 67\%$  of the *syn-CH}\_3\text{CHOO} produced in the SCI yield experiments would react with  $\text{SO}_2$ . Applying these (with the corresponding *syn* and *anti* yields shown in Table 4) corrections to  $\phi_{\text{min}}$  determines total SCI yields of 0.29 for *trans*-but-2-ene and 0.42 for *cis*-but-2-ene. These values both lie within the uncertainties in the SCI yields presented in Table 1 for the two but-2-ene systems.**

It is not practicable to assess the possible contribution of the water dimer to the SCI loss for  $\text{CH}_3\text{CHOO}$  because of the





**Table 4** Kinetic parameters derived for *syn*-CH<sub>3</sub>CHOO and *anti*-CH<sub>3</sub>CHOO from two-component fits to the *trans*-but-2-ene (T2B) and *cis*-but-2-ene (C2B) experiments (see Fig. 5). Also relative ( $\gamma$ ) and absolute ( $\phi$ ) yields of the two conformers

CH <sub>3</sub> CHOO	10 <sup>4</sup> $k_3/k_2$	10 <sup>14</sup> $k_3$ (cm <sup>3</sup> s <sup>-1</sup> )	10 <sup>-13</sup> $k_d/k_2$ (cm <sup>-3</sup> )	$k_d$ (s <sup>-1</sup> )	$\gamma^a$		$\phi$		Ref.	Conditions <sup>b</sup>
					T2B	C2B	T2B	C2B		
<i>syn</i>	—	— < 0.4 < 0.02	1.2 (±1.1)	288 (±275)	0.25	0.45	0.07	0.17	This work Taatjes <i>et al.</i> <sup>16</sup> Sheps <i>et al.</i> <sup>49</sup> Novelli <i>et al.</i> <sup>23</sup>	— 4 Torr 200 Torr 735 Torr
<i>anti</i>	3.5 (±3.1)	2.3 (±2.1) 1.0 (±0.4) 2.4 (±0.4)	—	—	0.75	0.55	0.21	0.21	This work Taatjes <i>et al.</i> <sup>16</sup> Sheps <i>et al.</i> <sup>49</sup>	— 4 Torr 200 Torr

<sup>a</sup>  $\gamma^{syn} = \phi^{syn}/\phi$ . <sup>b</sup> Experiments were conducted at atmospheric pressure unless stated otherwise and temperatures from 293 to 303 K.

number of free parameters that would result for a small dataset. However, theoretical predictions<sup>47</sup> suggest that this may be less important for CH<sub>3</sub>CHOO than for CH<sub>2</sub>OO, indicating  $k(\text{H}_2\text{O})_2/k(\text{H}_2\text{O})$  to be two orders of magnitude smaller for *anti*-CH<sub>3</sub>CHOO than for CH<sub>2</sub>OO.

### 3.4 (CH<sub>3</sub>)<sub>2</sub>COO

**3.4.1 Linear fit.** For (CH<sub>3</sub>)<sub>2</sub>COO a value of  $8.7 (\pm 2.5) \times 10^{-5}$  (Table 2) was obtained from a linear fit to the data in Fig. 3, excluding the experiment performed at the highest RH ([H<sub>2</sub>O] =  $1.6 \times 10^{17}$  cm<sup>-3</sup>) from the regression.  $(k_d + L)/k_2$  for (CH<sub>3</sub>)<sub>2</sub>COO was determined as  $63 (\pm 14) \times 10^{11}$  molecule per cm<sup>-3</sup>. These values can be placed on an absolute basis using the measurements of  $k_2(\text{syn-CH}_3\text{CHOO} + \text{SO}_2)$  reported by Taatjes *et al.*<sup>16</sup> as there are no reported  $k_2$  values for (CH<sub>3</sub>)<sub>2</sub>CHOO from direct experiments and (CH<sub>3</sub>)<sub>2</sub>COO is a *syn*-conformer (*i.e.* there is always a methyl group in a *syn* orientation to the terminal oxygen). This gives values for  $k_3$  ((CH<sub>3</sub>)<sub>2</sub>COO + H<sub>2</sub>O) of  $2.1 (\pm 0.6) \times 10^{-15}$  cm<sup>3</sup> s<sup>-1</sup> and for  $k_d$  of  $151 (\pm 35)$  s<sup>-1</sup> (Table 3).

Berndt *et al.*<sup>32</sup> have recently reported the  $k_3/k_2$  ratio for (CH<sub>3</sub>)<sub>2</sub>COO to be  $< 0.4 \times 10^{-5}$  (*i.e.* approximately a factor of 22 lower than the relative rate reported in this study). Theoretical predictions<sup>50</sup> also suggest  $k_3$  to be very slow,  $3.9 \times 10^{-17}$  cm<sup>3</sup> s<sup>-1</sup>. No measured values have been reported for  $k_d$  ((CH<sub>3</sub>)<sub>2</sub>COO), but a more facile overall decomposition than for CH<sub>2</sub>OO or the mean of the CH<sub>3</sub>CHOO isomers might be anticipated as the vinyl-hydroperoxide isomerisation channel<sup>26</sup> is always available.

**3.4.2 Additional oxidant.** In the case of the SCI formed from TME ozonolysis, (CH<sub>3</sub>)<sub>2</sub>COO, there is always a methyl group in a *syn* position to the carbonyl oxide moiety, thus the analysis presented in Section 3.3.2 for the CH<sub>3</sub>CHOO isomers does not apply. A possible alternative explanation for the observed behaviour (and possible contributor to the behaviour observed in the but-2-ene systems) is that there is a further oxidant (X) of SO<sub>2</sub>, in addition to the SCI, being formed during the ozonolysis reaction. If this oxidant reacts relatively slowly with H<sub>2</sub>O, it could give rise to the apparent 'two component' nature of the observations seen in Fig. 3. It may also provide an alternative explanation of the observed nature of the SO<sub>2</sub> loss from the but-2-ene experiments or could be occurring in addition to the effects of differing conformer reactivities.

Eqn (E9) (below) is an expanded version of (E2), in which we consider the contribution from a second SO<sub>2</sub> oxidant, making

the approximation that this species does not react appreciably with water vapour. In eqn (E9),  $f$  is the sum of  $f^{\text{SCI}}$  (the fraction of SCI reacting with SO<sub>2</sub>) and  $f^x$ , each multiplied by the relative yield of the total oxidant (*i.e.* SCI + X)  $\gamma^{\text{SCI}}$  and  $\gamma^x$ . Following the assumption of negligible H<sub>2</sub>O reactivity,  $(\text{dSO}_2/\text{dO}_3)_x$  in eqn (E9) can be derived from the SO<sub>2</sub> loss at the highest RH experiments (*i.e.* when all the SO<sub>2</sub> loss is attributed to X + SO<sub>2</sub>) of  $\sim 10$  ppbv. Therefore, loss of SO<sub>2</sub> from reaction with X, relative to the loss of O<sub>3</sub>  $(\text{dSO}_2/\text{dO}_3)_x$  is approximately 0.025.  $\phi$  represents the total oxidant yield (*i.e.*  $\phi_{\text{SCI}} + \phi_x$ ). Assuming that  $\gamma^x$  is not dominant ( $< 0.5$ ), then  $\phi$ , as calculated from correcting  $\phi_{\text{min}}$  as in Section 3.1, changes little (0.31–0.34) from the value presented in Table 1. Eqn (E10) is then an expanded version of eqn (E3) that includes the additional oxidant term.

$$f = \gamma^{\text{SCI}} f^{\text{SCI}} + \gamma^x f^x = \gamma^{\text{SCI}} f^{\text{SCI}} + \frac{1}{\phi} \left( \frac{\text{dSO}_2}{\text{dO}_3} \right)_x \quad (\text{E9})$$

$$[\text{SO}_2] \left( \frac{1}{f} - 1 \right)$$

$$= [\text{SO}_2] \left[ \left( \frac{\gamma^{\text{SCI}} [\text{SO}_2]}{[\text{SO}_2] + \frac{k_3}{k_2} [\text{H}_2\text{O}] + \frac{k_d}{k_2}} + \frac{1}{\phi} \left( \frac{\text{dSO}_2}{\text{dO}_3} \right)_x} \right)^{-1} - 1 \right] \quad (\text{E10})$$

Fig. 7 shows eqn (E10) fitted to the TME data from Fig. 3. It is not possible to determine unique values for the parameters included in eqn (E10) due to the degrees of freedom *vs.* the limited data set. The fit shown in Fig. 7 uses values of  $\phi = 0.34$ ,  $\gamma^{\text{SCI}} = 0.88$ ,  $k_3/k_2 = 6.7 \times 10^{-4}$  and  $k_d/k_2 = 1.2 \times 10^{12}$  cm<sup>-3</sup>. However, Fig. 7 does demonstrate that a two-oxidant system, as represented by eqn (E10), is able to describe the data within uncertainty.

Fig. 7 also includes a linear fit (*i.e.* eqn (E3)) to the full (CH<sub>3</sub>)<sub>2</sub>COO dataset (including the highest RH experiment). While it seems unlikely that the curvature observed in the data is a result of measurement error (as described in Section 3.1), this must be considered as a possibility for (CH<sub>3</sub>)<sub>2</sub>COO in light of the two conformer explanation not being applicable. The linear fit in Fig. 7 gives a  $k_3/k_2$  value of  $3.8 (\pm 3.2) \times 10^{-5}$  cm<sup>3</sup> s<sup>-1</sup>, a factor of two smaller than the  $k_3/k_2$  value presented in Table 2.



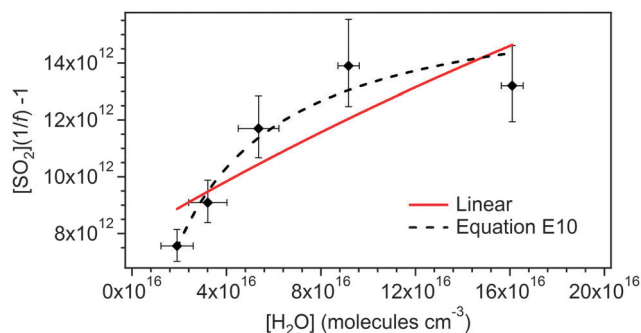


Fig. 7 Data for TME ozonolysis (as shown in Fig. 3), with fit to eqn (E10), and linear fit to the full dataset.

The most obvious candidate for an additional oxidant present to consume  $\text{SO}_2$  is OH. OH radicals are produced in the chamber, primarily (in the absence of sunlight and  $\text{NO}_x$ ) through the alkene + ozone reaction.<sup>11</sup> However cyclohexane was added in excess at the beginning of each experiment to act as an OH scavenger, such that  $\text{SO}_2$  reaction with OH was calculated to be  $\leq 1\%$  of the total chemical  $\text{SO}_2$  removal in all experiments. Other potential candidates for this oxidant species include the (stabilised) vinyl hydroperoxide (VHP) intermediate, a secondary ozonide (formed through an  $\text{SO}_2$ -SCI cyclic adduct), and dioxirane (Scheme 1).

Drozd *et al.*<sup>10</sup> have presented evidence for substantial VHP stabilisation (derived from the  $(\text{CH}_3)_2\text{COO}$  CI) at pressures of a few hundred Torr, with a lifetime of the order of a few hundred milliseconds with respect to decomposition to form OH, providing scope for bimolecular reactions of this species to occur. This would be consistent with the kinetic observations presented here: a small yield in the systems with *syn*-SCIs, while for ethene, no VHP intermediate is available, and the standard chemistry ((R1)–(R4)) can be used to satisfactorily reproduce the observations. However, no significant  $\text{SO}_2$  reactivity is known for the peroxide or alkene functionalities present in the closed shell VHP in isolation, hence it may be surprising if this species reacted rapidly with  $\text{SO}_2$ , although theoretical studies have suggested that the VHP may react with  $\text{H}_2\text{O}$ .<sup>23</sup>

Secondary ozonide species, formed as an adduct from the SCI +  $\text{SO}_2$  reaction, have been suggested to account for the observed isotopic exchange in alkene–ozone– $\text{SO}_2$  systems,<sup>25</sup> and are suggested to have lifetimes of seconds or longer.<sup>19</sup> Such a secondary ozonide could react with a further  $\text{SO}_2$  molecule (*i.e.* a two-component secondary ozonide catalysed oxidation route for  $\text{SO}_2$  to  $\text{SO}_3$  conversion), however a substantial humidity dependence to the overall process may still be anticipated (on the basis of SCI removal through the SCI +  $\text{H}_2\text{O}$  reaction), which is not observed here.

The ‘hot acid/ester channel’ (rearrangement and decomposition *via* a dioxirane intermediate) is the dominant isomerisation route available for *anti*-SCIs. Although the hydroperoxide channel is the principal isomerisation route for *syn*-SCIs, the ester mechanism is also available,<sup>25</sup> and it is likely that a small proportion of the *syn*-CI will isomerise through this channel to form a dioxirane. Dioxiranes are known to be highly reactive and selective oxidising agents,<sup>51,52</sup> and have a particular affinity

for sulphur compounds.<sup>53</sup> Additional oxidation of  $\text{SO}_2$  by the dioxirane, over and above that arising directly from reaction with the SCI, could then explain the observed behaviour of  $\text{SO}_2$  in the TME experiments (and contribute to the behaviour observed for the but-2-ene systems). For the small CI  $\text{CH}_2\text{OO}$ , formed in the ethene system, it has been predicted that the dioxirane formed is considerably less stable than the methyl substituted dioxiranes formed from but-2-ene and TME ozonolysis, and furthermore will decompose promptly due to chemical activation.

The possibility of non-CI products of the ozonolysis system being responsible for some of the observed  $\text{SO}_2$  oxidation has been suggested previously as an alternative (or additional) explanation for the observed behaviour of  $\text{SO}_2$  in the atmosphere.<sup>1,54,55</sup> In their laboratory study Berndt *et al.*<sup>19</sup> note that their data were not perfectly described by a model in which a single (SCI related)  $\text{SO}_2$  oxidation process was assumed, and commented that the  $\text{SO}_2$  oxidation in ozonolysis systems may in fact be more complex. Taatjes *et al.*<sup>56</sup> have recently suggested that these data<sup>19</sup> are consistent with a two-component oxidation system, either two processes removing  $\text{SO}_2$  in parallel (as described above), or through a sequential two-step  $\text{SO}_2$  removal mechanism, such as the secondary ozonide route outlined above. However, this latter mechanism cannot (in isolation) account for the observations presented here.

The presence of an additional oxidant would have implications for the role of alkene ozonolysis in oxidation of trace gases in the atmosphere. If an oxidant is being formed that reacts slowly with  $\text{H}_2\text{O}$  then this, perhaps in addition to SCI, may contribute to the additional (non-OH)  $\text{SO}_2$  oxidation observed in recent field experiments.<sup>1</sup> Further investigation of this possibility is needed.

As for  $\text{CH}_3\text{CHOO}$ , the analysis performed in this section has implications for the determination of the SCI ( $(\text{CH}_3)_2\text{COO}$ ) yield. Using the value of  $k_d$  derived from the linear fit to all the data shown in Fig. 7 would indicate an SCI yield of 0.33. Using the value of  $k_d$  derived from the ‘additional oxidant fit in Fig. 7, and taking into account that  $\sim 10$  ppb of the  $\text{SO}_2$  loss in the high  $\text{SO}_2$  experiment would be attributed to reaction with the additional oxidant rather than the SCI, determines a slightly lower  $\varphi_{\text{min}}$  of 0.23, and a corrected yield of 0.32, very similar to that shown in Table 1. Both of these possible alternative SCI yields lie within the uncertainties in the SCI yield from TME ozonolysis presented in Table 1.

As for  $\text{CH}_3\text{CHOO}$ , it is not possible to quantitatively consider the contribution of the water dimer to the SCI loss given the limited data, but theory<sup>53</sup> predicts  $k(\text{H}_2\text{O})_2/k(\text{H}_2\text{O})$  to be three orders of magnitude smaller than that for  $\text{CH}_2\text{OO}$  suggesting that reaction with the water dimer would be unimportant for  $(\text{CH}_3)_2\text{COO}$  at typical atmospheric boundary layer  $[\text{H}_2\text{O}]$ .

## 4. Atmospheric implications

The derived values for  $k_3$  reported in Table 3 correspond to loss rates for reaction of SCI with  $\text{H}_2\text{O}$  in the atmosphere of  $650 \text{ s}^{-1}$  for  $\text{CH}_2\text{OO}$ ,  $\sim 3500 \text{ s}^{-1}$  for  $\text{CH}_3\text{CHOO}$  and  $\sim 1050 \text{ s}^{-1}$  for  $(\text{CH}_3)_2\text{COO}$



(assuming  $[\text{H}_2\text{O}] = 5 \times 10^{17}$  molecules per  $\text{cm}^{-3}$ , equivalent to an RH of 65% at 298 K). Comparing this to the derived  $k_d$  values it is seen that reaction with  $\text{H}_2\text{O}$  is predicted to be the main sink for SCI in the atmosphere, but also that loss through decomposition cannot be neglected for some SCIs – contributing on the order of 0–1% for  $\text{CH}_3\text{CHOO}$  and 13% for  $(\text{CH}_3)_2\text{COO}$ .

An estimate of a mean steady state SCI concentration in the background atmospheric boundary layer can then be calculated using eqn (E11).

$$[\text{SCI}] = \frac{[\text{Alkene}][\text{O}_3]k_1\phi}{k_3[\text{H}_2\text{O}] + k_d} \quad (\text{E11})$$

Using the data given below, a steady state SCI concentration of  $1.7 \times 10^3$  molecules per  $\text{cm}^{-3}$  is estimated for an ozonolysis source (noting that other potential atmospheric sources of SCI exist, e.g. photolysis of alkyl-iodides in the marine boundary layer, and sinks, e.g. reaction with  $\text{NO}$  and  $\text{NO}_2$ ). This assumes an ozone mixing ratio of 40 ppbv, an alkene mixing ratio of 2 ppbv,  $\phi$  of 0.35, and mean reaction rate constants  $k_1$  (alkene–ozone) of  $1 \times 10^{-16} \text{ cm}^3 \text{ s}^{-1}$ ;  $k_2$  (SCI +  $\text{SO}_2$ ) of  $3.5 \times 10^{-11} \text{ cm}^3 \text{ s}^{-1}$ ,  $k_3$  (SCI +  $\text{H}_2\text{O}$ ) of  $2 \times 10^{-15} \text{ cm}^3 \text{ s}^{-1}$ ,  $k_d$  of  $30 \text{ s}^{-1}$  with  $[\text{H}_2\text{O}]$  of  $5 \times 10^{17} \text{ cm}^{-3}$  (RH  $\sim$  65%).

However, in the case of  $\text{CH}_3\text{CHOO}$  the data shown in Fig. 3, and the discussion above, indicate contributions from multiple species – *syn*- and *anti*-conformers with contrasting behaviour. It is clear that the burden of  $\text{CH}_3\text{CHOO}$  in the atmosphere would be better described by considering these two fractions of  $\text{SO}_2$  loss separately. Eqn (E12) expands eqn (E11) to treat the two conformers separately, where  $[\text{SCI}] = [\text{anti-SCI}] + [\text{syn-SCI}]$ , making the same assumptions as for the analysis of  $\text{CH}_3\text{CHOO}$  in eqn (E5) and (E6).  $k_3^{\text{anti}}$  is estimated to be  $1 \times 10^{-14} \text{ cm}^3 \text{ s}^{-1}$  (taking into account that  $\text{CH}_2\text{OO}$  is considered as an *anti*-SCI in this analysis and that the derived  $k_3(\text{CH}_2\text{OO})$  is more than an order of magnitude smaller than the derived  $k_3(\text{CH}_3\text{CHOO})$  of  $2.3 \times 10^{-14} \text{ cm}^3 \text{ s}^{-1}$ ),  $k_5^{\text{syn}}$  is assumed to be  $200 \text{ s}^{-1}$  and  $\phi^{\text{anti}} = \phi^{\text{syn}} = 0.175$ . Additionally the *anti*-SCI + water dimer reaction is also considered, using a value of  $5.6 \times 10^{-13} \text{ cm}^3 \text{ s}^{-1}$  as derived for  $\text{CH}_2\text{OO}$  in this work.

$$[\text{SCI}] = [\text{Alkene}][\text{O}_3]k_1 \left( \frac{\phi^{\text{anti}}}{k_3^{\text{anti}}[\text{H}_2\text{O}] + k_5^{\text{anti}}K_p[\text{H}_2\text{O}]^2} + \frac{\phi^{\text{syn}}}{k_d^{\text{syn}}} \right) \quad (\text{E12})$$

Using these values in eqn (E12) determines  $[\text{anti-SCI}] = 164$  molecules per  $\text{cm}^{-3}$  and  $[\text{syn-SCI}] = 4.4 \times 10^3$  molecules per  $\text{cm}^{-3}$ . The formation of an additional oxidant during alkene ozonolysis would be expected to have a similar effect to the two component contribution presented in eqn (E12) based on the apparent yields from the experiments presented here. From this analysis the atmospheric SCI burden is seen to likely be dominated by *syn*-SCI since this term is at least an order of magnitude greater than the *anti*-SCI term.

A typical diurnal loss rate of  $\text{SO}_2$  to  $\text{OH}$  ( $k_{\text{OH}} \times [\text{OH}]$ ) is  $9 \times 10^{-7} \text{ s}^{-1}$ ,<sup>15</sup> while the  $\text{SO}_2$  loss rate due to reaction with SCI, using the values derived from eqn (E12), would be  $1.2 \times 10^{-7} \text{ s}^{-1}$ . This suggests, for the conditions and assumptions given above, the

loss of  $\text{SO}_2$  to SCI to be about 13% of loss to  $\text{OH}$ . This analysis neglects additional chemical sinks for SCI, which would reduce SCI abundance but are unlikely to be competitive with the two main SCI loss processes identified herein. SCI concentrations are expected to vary greatly depending on the local environment, e.g. alkene abundance may be considerably higher (and with a different reactive mix of alkenes) in a forested environment, compared to a rural background environment. The majority of the SCI burden, particularly in forested regions, is likely to be dominated by larger SCI derived from ( $\text{C}_5$ ) isoprene and ( $\text{C}_{10}$ ) monoterpenes. The chemistry of these species could differ greatly from the small SCI reported here (which we have found to be structure specific, even for small alkene systems), especially for tethered SCI derived from ozonolysis of internal double bonds within (for example) some monoterpenes. It is clear that the total SCI loss rate is dependent upon SCI identity and configuration, and that further work is required to quantify speciated SCI in the atmosphere, and to accurately calculate SCI concentrations for use in atmospheric modelling.

## 5. Conclusions

It has been shown that at relatively low  $[\text{H}_2\text{O}]$  ( $< 1 \times 10^{17} \text{ cm}^{-3}$ ) the loss of  $\text{SO}_2$  in the presence of four ozone–alkene systems: ethene, *cis*-but-2-ene, *trans*-but-2-ene and 2,3-dimethyl-but-2-ene significantly decreases with increasing water vapour. This is consistent with production of a stabilised Criegee intermediate from the ozonolysis reaction and subsequent reaction of this species with  $\text{SO}_2$  and  $\text{H}_2\text{O}$ . Competition between  $\text{H}_2\text{O}$  and  $\text{SO}_2$  for reaction with the SCI leads to the observed relationship which is sensitive to water vapour abundance over a relatively narrow range of RH. Derived kinetic data for these ozonolysis systems shows that the reaction rates are dependent on the structure of the SCI. At  $[\text{H}_2\text{O}] > 1 \times 10^{17} \text{ cm}^{-3}$  the  $\text{SO}_2$  loss in the presence of *cis*- and *trans*-but-2-ene, and 2,3-dimethyl-but-2-ene appears to show a reduced dependence upon  $\text{H}_2\text{O}$ . The results suggest that there is an  $\text{H}_2\text{O}$  dependent and an  $\text{H}_2\text{O}$  independent fraction to the observed  $\text{SO}_2$  loss in these systems. These two fractions may be attributable to differing kinetics of the two conformers produced in but-2-ene ozonolysis or to other oxidant products of the alkene ozonolysis reaction. This observation means that SCI structure must be considered in atmospheric modelling of SCI production from alkene ozonolysis, and suggests that the atmospheric SCI burden (and hence the oxidation of trace gases) will be dominated by *syn*-SCI.

This work provides constraints on the behaviour of SCI formed through alkene ozonolysis under conditions relevant to the atmospheric boundary layer, but also highlights the complex nature and incomplete current understanding of the ozonolysis system. Further research is needed to definitively quantify the impact of this chemistry upon atmospheric oxidation.

## Acknowledgements

The assistance of the EUPHORE staff is gratefully acknowledged. Marie Camredon, Stephanie La and Mat Evans are thanked for



helpful discussions. This work was funded by EU FP7 EUROCHAMP 2 Transnational Access activity (E2-2012-05-28-0077), the UK NERC (NE/K005448/1) and Fundacion CEAM. Fundación CEAM is partly supported by Generalitat Valenciana, and the projects GRACCIE (Consolider-Ingenio 2010) and FEEDBACKS (Prometeo – Generalitat Valenciana). EUPHORE instrumentation is partly funded by the Spanish Ministry of Science and Innovation, through INNPLANTA project: PCT-440000-2010-003. LV is supported by the Max Planck Graduate Center with the Johannes Gutenberg-Universität Mainz (MPGC).

## Notes and references

- R. L. Mauldin III, T. Berndt, M. Sipilä, P. Paasonen, T. Petäjä, S. Kim, T. Kurtén, F. Stratmann, V.-M. Kerminen and M. Kulmala, *Nature*, 2012, **488**, 193.
- G. Sarwar, K. Fahey, R. Kwok, R. C. Gilliam, S. J. Roselle, R. Mathur, J. Xue, J. Yu and W. P. L. Carter, *Atmos. Environ.*, 2013, **68**, 186.
- P. Forster and V. Ramaswamy, *et al.*, *IPCC 4*, 2007, ch. 2, vol. 160.
- R. A. Cox and S. A. Penkett, *Nature*, 1971, **230**, 321.
- R. Criegee and G. Wenner, *Liebigs Ann. Chem.*, 1949, **564**, 9.
- D. Johnson and G. Marston, *Chem. Soc. Rev.*, 2008, **37**, 699.
- H. Niki, P. D. Maker, C. M. Savage, L. P. Breitenbach and M. D. Hurley, *J. Phys. Chem.*, 1987, **91**, 941.
- R. I. Martinez and J. T. Herron, *J. Phys. Chem.*, 1987, **91**, 946.
- G. T. Drozd, J. Kroll and N. M. Donahue, *J. Phys. Chem. A*, 2011, **115**, 161.
- G. T. Drozd and N. M. Donahue, *J. Phys. Chem. A*, 2011, **115**, 4381.
- M. S. Alam, A. R. Rickard, M. Camredon, K. P. Wyche, T. Carr, K. E. Hornsby, P. S. Monks and W. J. Bloss, *J. Phys. Chem. A*, 2013, **117**, 12468.
- K. Izumi, M. Mizuochi, K. Murano and T. Fukuyama, *Atmos. Environ.*, 1987, **21**, 1541.
- J. G. Calvert, R. Atkinson, J. A. Kerr, S. Madronich, G. K. Moortgat, T. J. Wallington and G. Yarwood, *The Mechanisms of Atmospheric Oxidation of the Alkenes*, Oxford University Press, New York, 2000.
- C. A. Taatjes, G. Meloni, T. M. Selby, A. J. Trevitt, D. L. Osborn, C. J. Percival and D. E. Shallcross, *J. Am. Chem. Soc.*, 2008, **130**, 11883.
- O. Welz, J. D. Savee, D. L. Osborn, S. S. Vasu, C. J. Percival, D. E. Shallcross and C. A. Taatjes, *Science*, 2012, **335**, 204.
- C. A. Taatjes, O. Welz, A. J. Eskola, J. D. Savee, A. M. Scheer, D. E. Shallcross, B. Rotavera, E. P. F. Lee, J. M. Dyke, D. W. K. Mok, D. L. Osborn and C. J. Percival, *Science*, 2013, **340**, 177.
- D. Stone, M. Blitz, L. Daubney, N. U. M. Howes and P. Seakins, *Phys. Chem. Chem. Phys.*, 2014, **16**, 1139.
- B. Ouyang, M. W. McLeod, R. L. Jones and W. J. Bloss, *Phys. Chem. Chem. Phys.*, 2013, **15**, 17070.
- T. Berndt, T. Jokinen, R. L. Mauldin III, T. Petaja, H. Herrmann, H. Junninen, P. Paasonen, D. R. Worsnop and M. Sipilä, *J. Phys. Chem. Lett.*, 2012, **3**, 2892.
- L. Vereecken, H. Harder and A. Novelli, *Phys. Chem. Chem. Phys.*, 2012, **14**, 14682.
- J. R. Pierce, M. J. Evans, C. E. Scott, S. D. D'Andrea, D. K. Farmer, E. Swietlicki and D. V. Spracklen, *Atmos. Chem. Phys.*, 2013, **13**, 3163.
- M. Olzmann, E. Kraka, D. Cremer, R. Gutbrod and S. Andersson, *J. Phys. Chem. A*, 1997, **101**, 9421.
- A. Novelli, L. Vereecken, J. Lelieveld and H. Harder, *Phys. Chem. Chem. Phys.*, 2014, **16**, 19941.
- K. T. Kuwata, M. R. Hermes, M. J. Carlson and C. K. Zogg, *J. Phys. Chem. A*, 2010, **114**, 9192.
- J. T. Herron, R. I. Martinez and R. E. Huie, *Int. J. Chem. Kinet.*, 1982, **14**, 201.
- J. D. Fenske, A. S. Hasson, A. W. Ho and S. E. Paulson, *J. Phys. Chem. A*, 2000, **104**, 9921.
- J. H. Kroll, S. R. Sahay, J. G. Anderson, K. L. Demerjian and N. M. Donahue, *J. Phys. Chem. A*, 2001, **105**, 4446.
- J. M. Beames, F. Liu, L. Lu and M. I. Lester, *J. Am. Chem. Soc.*, 2012, **134**, 19104.
- J. M. Beames, F. Liu, L. Lu and M. I. Lester, *J. Chem. Phys.*, 2013, **138**, 244307.
- K. H. Becker, *EUPHORE: Final Report to the European Commission, Contract EV5V-CT92-0059*, Bergische Universität, Wuppertal, Germany, 1996.
- M. S. Alam, M. Camredon, A. R. Rickard, T. Carr, K. P. Wyche, K. E. Hornsby, P. S. Monks and W. J. Bloss, *Phys. Chem. Chem. Phys.*, 2011, **13**, 11002.
- T. Berndt, T. Jokinen, M. Sipilä, R. L. Mauldin, H. Herrmann, F. Stratmann, H. Junninen and M. Kulmala, *Atoms. Environ.*, 2014, **89**, 603.
- S. M. Saunders, M. E. Jenkin, R. G. Derwent and M. J. Pilling, *Atmos. Chem. Phys.*, 2003, **3**, 161.
- H. Niki, P. D. Maker, C. M. Savage and L. P. Breitenbach, *J. Phys. Chem.*, 1981, **85**, 1024.
- S. Hatakeyama, H. Kobayashi and H. Akimoto, *J. Phys. Chem.*, 1984, **88**, 4736.
- O. Horie and G. K. Moortgat, *Atmos. Environ., Part A*, 1991, **24**, 1881.
- P. Neeb, O. Horie and G. K. Moortgat, *Int. J. Chem. Kinet.*, 1996, **28**, 721.
- A. S. Hasson, G. Orzechowska and S. E. Paulson, *J. Geophys. Res.*, 2001, **106**, 34131.
- A. R. Rickard, D. Johnson, C. D. McGill and G. Marston, *J. Phys. Chem. A*, 1999, **103**, 7656.
- H. Niki, P. D. Maker, C. M. Savage and L. P. Breitenbach, *Chem. Phys. Lett.*, 1977, **46**, 327.
- R. A. Cox and S. A. Penkett, *J. Chem. Soc., Faraday. Trans.*, 1972, **68**, 1735.
- H. G. Kjaergaard, T. Kurtén, L. B. Nielsen, S. Jørgensen and P. O. Wennberg, *J. Phys. Chem. Lett.*, 2013, **4**, 2525.
- L. Vereecken, H. Harder and A. Novelli, *Phys. Chem. Chem. Phys.*, 2014, **16**, 4039.
- C. A. Taatjes, O. Welz, A. J. Eskola, J. D. Savee, D. L. Osborn, E. P. F. Lee, J. M. Dyke, D. W. K. Mok, D. E. Shallcross and C. J. Percival, *Phys. Chem. Chem. Phys.*, 2012, **14**, 10391.
- O. Welz, A. J. Eskola, L. Sheps, B. Rotavera, J. D. Savee, A. M. Scheer, D. L. Osborn, D. Lowe, A. Murray Booth,





- P. Xiao, M. Anwar H. Kahn, C. J. Percival, D. E. Shallcross and C. A. Taatjes, *Angew. Chem., Int. Ed.*, 2014, **18**, 4547.
- 46 T. Berndt, J. Voigtländer, F. Stratmann, H. Junninen, R. L. Mauldin III, M. Sipilä, M. Kulmala and H. Herrmann, *Phys. Chem. Chem. Phys.*, 2014, **16**, 19130.
- 47 A. B. Ryzhkov and P. A. Ariya, *Phys. Chem. Chem. Phys.*, 2004, **6**, 5042.
- 48 Y. Scribano, N. Goldman, R. J. Saykally and C. Leforestier, *J. Phys. Chem. A*, 2006, **110**, 5411.
- 49 L. Sheps, A. M. Scully and K. Au, *Phys. Chem. Chem. Phys.*, 2014, **16**, 26701.
- 50 J. M. Anglada, J. Gonzalez and M. Torrent-Sucarrat, *Phys. Chem. Chem. Phys.*, 2011, **13**, 13034.
- 51 W. Adam, R. Curci and J. O. Edwards, *Acc. Chem. Res.*, 1989, **22**, 205.
- 52 R. W. Murray, *Chem. Rev.*, 1989, **89**, 1187.
- 53 R. Curci, A. Dinoi and M. F. Rubino, *Pure Appl. Chem.*, 1995, **67**, 811.
- 54 D. Heard, *Nature*, 2012, **488**, 164.
- 55 J. Prousek, *Chem. Listy*, 2009, **103**, 271.
- 56 C. A. Taatjes, D. E. Shallcross and C. J. Percival, *Phys. Chem. Chem. Phys.*, 2013, **16**, 1704.

